Frontiers of Materials Science

Electronic Supplementary Material

Layered NiFe-LDH grown on porous carbon nested in nickel foam or nickel net toward oxygen evolution reaction at large current density

Xinyu Lei[1], Enhui Hou[1], Tian Xia (✉)[2], and Jingping Wang (✉)[1]

1 Key Laboratory of Superlight Material and Surface Technology (Ministry of Education), College of Materials Science and Chemical Engineering, Harbin Engineering University, Harbin 150001, China

2 Key Laboratory of Functional Inorganic Material Chemistry (Ministry of Education), School of Chemistry, Chemical Engineering and Materials, Heilongjiang University, Harbin 150080, China

E-mails: wangjingping@hrbeu.edu.cn (J.W.), xiatian@hlju.edu.cn (T.X.)

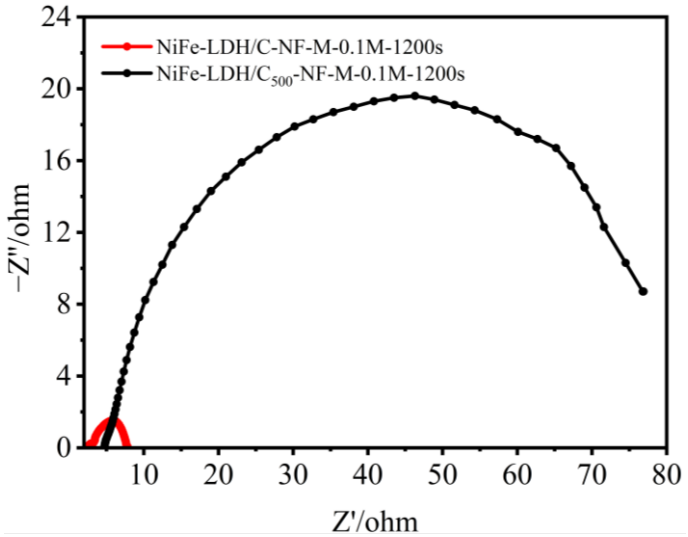

Fig. S1 Nyquist plots of NiFe-LDH/C-NF-M-0.1-1200 and NiFe-LDH/C_{500}-NF-M-0.1-1200 at 1.45 V *vs.* RHE.

Before carbonization, PAN needs to be stabilized. The nitrile groups of PAN undergo cyclization events during the stabilization phase, transforming the initial linear molecular chains into a thermally stable ladder-type structure that keeps them from melting during the subsequent carbonization 0. According to earlier research, PAN cyclization mostly takes place in the temperature range of 268–279 °C under a nitrogen environment 0, and a stabilization temperature of 280 °C has been commonly accepted in the literature [S3–S4]. As a result, 280 °C was chosen for PAN stabilization in this investigation.

To evaluate the effect of carbonization temperature on electrical conductivity, a control sample (C_{500}-NF-M) was prepared by carbonizing the stabilized PAN film at 500 °C, while all other preparation conditions were kept identical to those used for the main sample carbonized at 800 °C (denoted as C-NF-M). After electrodepositing NiFe-LDH catalysts on both substrates, their electrochemical impedance spectra (EIS) were examined (Fig. S1). The charge transfer resistance (R_{ct}) of NiFe-LDH/C_{500}-NF-M-0.1-1200 (76.8 Ω) is around 15.6 times greater than that of NiFe-LDH/C-NF-M-0.1-1200, suggesting that carbonization at 500 °C is not enough to completely transform the

organic film into a conductive carbon framework. On the other hand, complete carbonization and greatly increased electrical conductivity are made possible by carbonization at 800 °C. Therefore, 800 °C was chosen as the carbonization temperature in this work, in accordance with earlier publications [S3–S5].

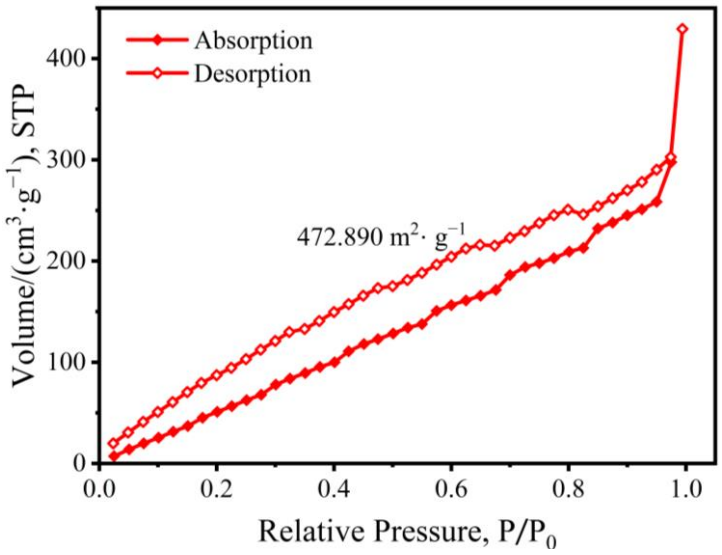

Fig. S2 Nitrogen adsorption–desorption isotherms of C-NF.

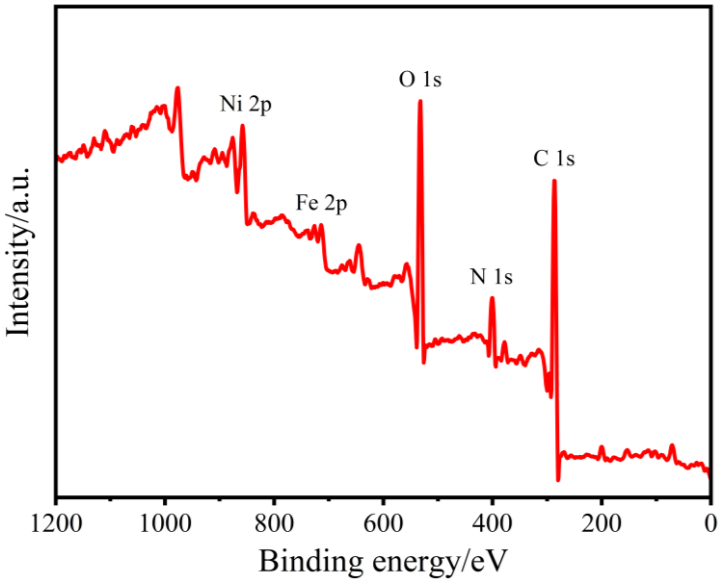

Fig. S3 XPS survey spectrum of NiFe-LDH/C-NF-M-0.1-1200.

The loading amount of NiFe-LDH was determined using the mass difference method. First, the initial mass of the C-NF-M substrates was precisely measured and noted as x. After electrodeposition, the substrates loaded with NiFe-LDH were washed, dried, and then their mass was accurately weighed and noted as y. Considering that adsorbed substances on the substrate may also contribute to the mass increase during electrodeposition, a blank experiment was conducted to evaluate the percentage of mass increase caused by adsorption, which was defined as z. Therefore, the actual loading amount of NiFe-LDH can be calculated using the following equation:

$$\text{Loading amount} = y - x - z \cdot x \quad \text{(S1)}$$

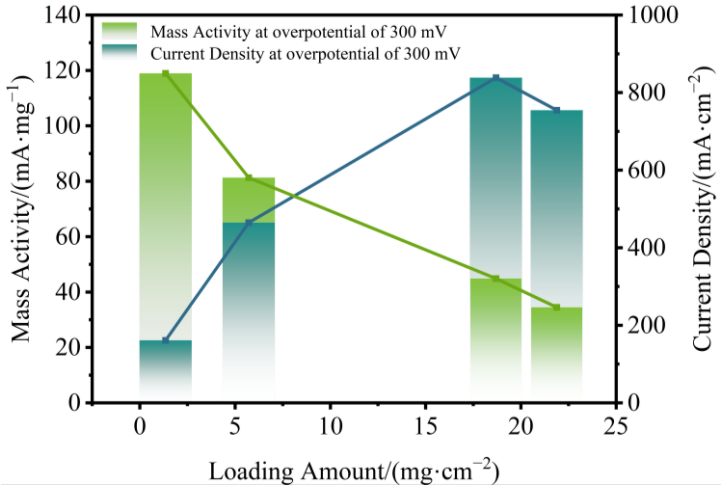

Fig. S4 Relationship between NiFe-LDH loading amount and OER activity. The mass activity (left axis) reflects the utilization efficiency of active sites, while the current density (right axis) represents the overall electrode performance.

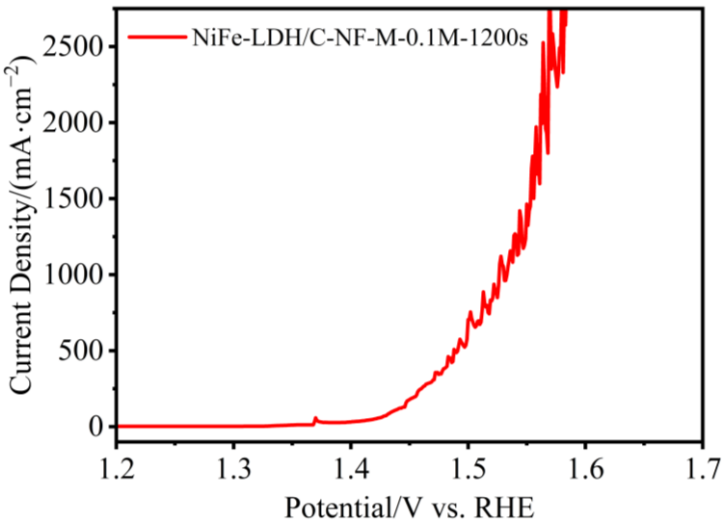

Fig. S5 OER performance of NiFe-LDH/C-NF-M-0.1-1200.

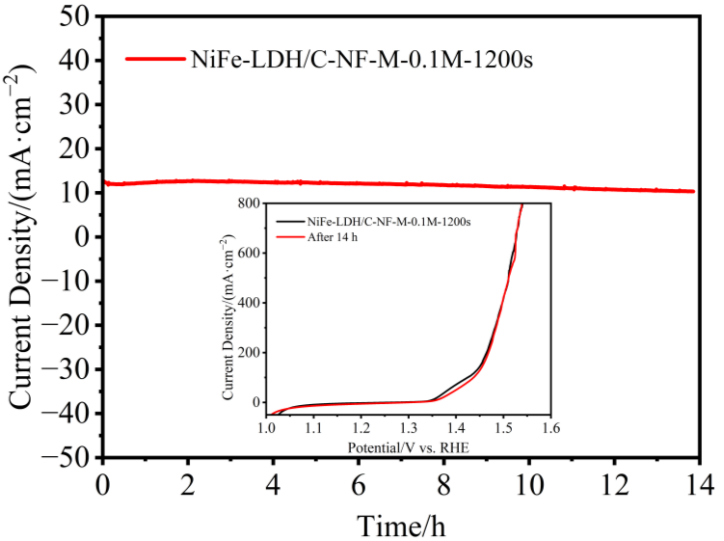

Fig. S6 The chronoamperometric response at 10 mA·cm^{-2}.

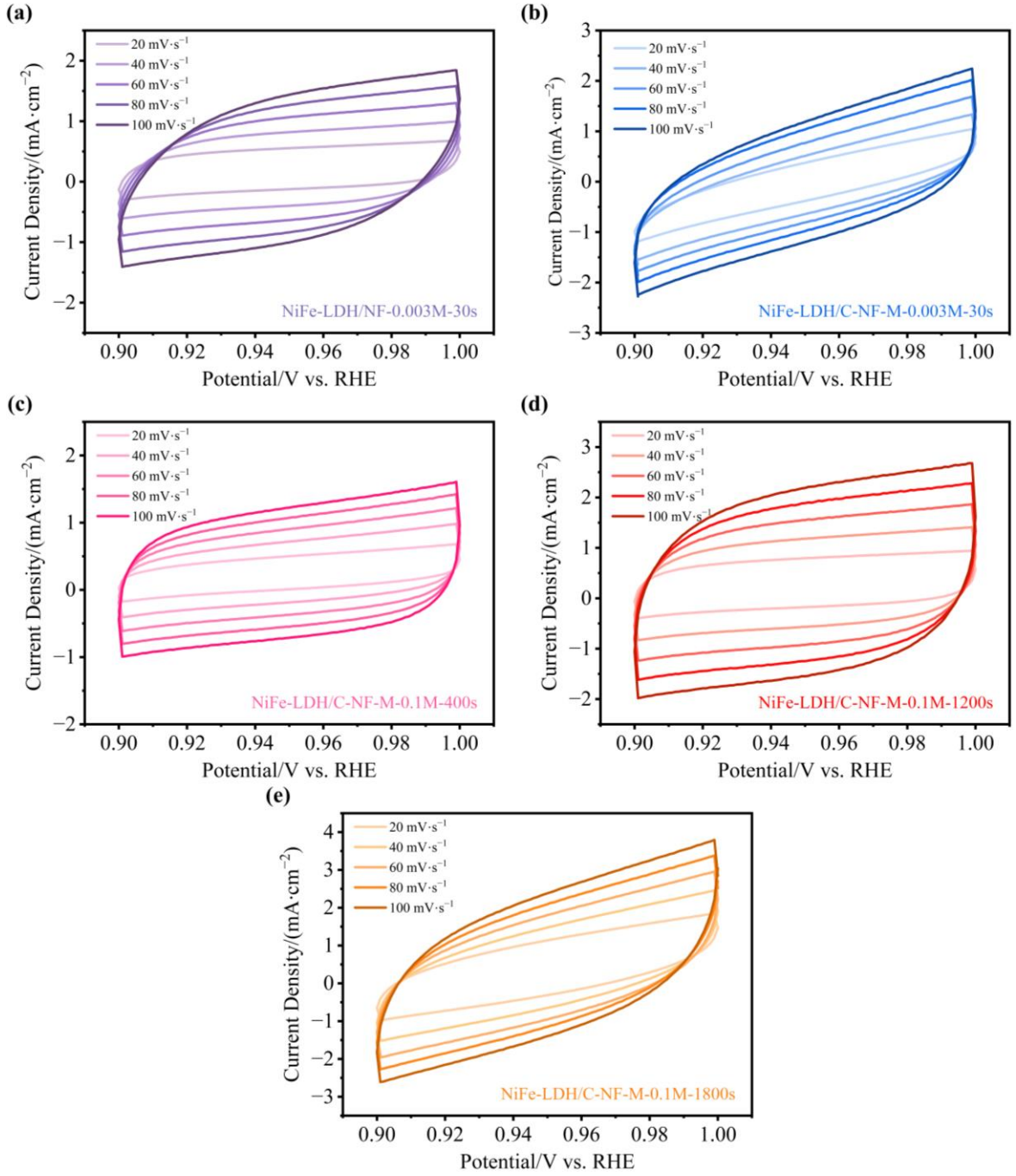

Fig. S7 CV curves of **(a)** NiFe-LDH/NF-0.003-30, **(b)** NiFe-LDH/C-NF-M-0.003-30, **(c)** NiFe-LDH/C-NF-M-0.1-400, **(d)** NiFe-LDH/C-NF-M-0.1-1200, and **(e)** NiFe-LDH/C-NF-M-0.1-1800 at different scan rates in non-faradaic region.

Table S1 Electrochemical performances of NiFe-LDH/C-NF-M at different NiFe-LDH loadings

Catalyst	Loading /(mg·cm^{-2})	η_{10} /mV	Tafel slope /(mV·dec^{-1})	J_{300} /(mA·cm^{-2})	MA_{300} /(mA·mg^{-1})
NiFe-LDH/C-NF-M-0.003-30	1.35	238	51.44	161.08	118.94
NiFe-LDH/C-NF-M-0.1-400	5.72	198	55.71	464.67	81.28
NiFe-LDH/C-NF-M-0.1-1200	18.69	189	44.19	838.33	44.85
NiFe-LDH/C-NF-M-0.1-1800	21.88	203	48.41	754.58	34.49

Notes: η_{10} refers to the overpotential at 10 mA·cm^{-2}; J_{300} refers to the current density at an overpotential of 300 mV; MA_{300} refers to mass activity at an overpotential of 300 mV.

Table S2 Comparison of electrocatalytic OER performance of recently reported non-precious metal electrocatalysts in 1 mol·L^{-1} KOH electrolyte

Catalyst	η/mV@100 mA·cm^{-2}	Tafel slope/(mV·dec^{-1})	Ref.
NiFe-LDH/C-NF-M-0.1-1200	230	44.19	This work
NiFeLa-LDH/v-MXene/NF	231	40	0
Co-CH@NiFe-LDH/NF	232	56	0
NiSe@CoFe LDH/NF	236	90.3	0
NiFe-LDH/$NiCo_2O_4$/NF	236	57.6	0
CoP@NiFe LDH/NF	238	35.4	0
Ni_2Fe-LDH/$FeNi_2S_4$/NF	240	29.4	0
N-CDs/NiFe-LDH/NF	260	43.4	0
$NiV_{0.1}$-BLDH/NiCoP/NF	268	155.3	0
CoO-Co_4N@NiFe-LDH/NF	270	39	0
Mo-NiS_x@NiFe LDH/NF	271	44.41	0
NiSe@NiMn LDH/NF	287	164.7	0
$NiCoS_x$-0.4/NF	289	75.4	0
Ni-FeLDH@$MnCO_3$/NF	328	45	0
FQD/CoNi-LDH/NF	368	94	0

References

[S1] Hameed N, Sharp J, Nunna S, et al. Structural transformation of polyacrylonitrile fibers during stabilization and low temperature carbonization. Polymer Degradation and Stability, 2016, 128: 39–45

[S2] Liu H C, Zhang S, Yang J L, et al. Preparation, stabilization and carbonization of a novel polyacrylonitrile-based carbon fiber precursor. Polymers, 2019, 11(7): 1150–1150

[S3] Gao K, Shen M X, Duan C, et al. Co-N-doped directional multichannel PAN/CA-based electrospun carbon nanofibers as high-efficiency bifunctional oxygen electrocatalysts for Zn–air batteries. ACS Sustainable Chemistry & Engineering, 2021, 9: 17068–17077

[S4] Li M X, Wang H Y, Zhu W D, et al. RuNi nanoparticles embedded in N-doped carbon nanofibers as a robust bifunctional catalyst for efficient overall water splitting. Advanced Science, 2020, 7(2): 1901833

[S5] Sun J X, Ge Q Z, Guo L, et al. Nitrogen doped carbon fibers derived from carbonization of electrospun polyacrylonitrile as efficient metal-free HER electrocatalyst. International Journal of Hydrogen Energy, 2020, 45(7): 4035–4042

[S6] Yu M Z, Zheng J Q, Guo M. La-doped NiFe-LDH coupled with hierarchical vertically aligned MXene frameworks for efficient overall water splitting. Journal of Energy Chemistry, 2022, 70: 472–479

[S7] Cao S, Huang H J, Shi K, et al. Engineering superhydrophilic/superaerophobic hierarchical structures of Co-CH@NiFe-LDH/NF to boost the oxygen evolution reaction. Chemical Engineering Journal, 2021, 422: 130123

[S8] Nie F, Li Z, Dai X P, et al. Interfacial electronic modulation on heterostructured NiSe@CoFe LDH nanoarrays for enhancing oxygen evolution reaction and water splitting by facilitating the deprotonation of OH to O. Chemical Engineering Journal, 2022, 431: 134080

[S9] Xing Z H, Zhao Y, Wang Y H, et al. Boosting charge transfer via interface charge reconstruction between amorphous NiFe-LDH and crystalline $NiCo_2O_4$ for efficient alkaline water/seawater oxidation. Nano Research, 2024, 17(6): 4856–4863

[S10] Gao G H, Zhao R Z, Wang Y J, et al. Core–shell heterostructure engineering of CoP nanowires coupled

NiFe LDH nanosheets for highly efficient water/seawater oxidation. Chinese Chemical Letters, 2024, 35(8): 109181

[S11] Tan L, Yu J T, Wang C, et al. Partial sulfidation strategy to NiFe-LDH@$FeNi_2S_4$ heterostructure enable high-performance water/seawater oxidation. Advanced Functional Materials, 2022, 32(29): 2200951

[S12] Ding P, Song H Q, Chang J W, et al. N-doped carbon dots coupled NiFe-LDH hybrids for robust electrocatalytic alkaline water and seawater oxidation. Nano Research, 2022, 15(8): 7063–7070

[S13] Gao T Q, Zhou Y Q, Zhao X J, et al. Borate anion-intercalated NiV-LDH nanoflakes/NiCoP nanowires heterostructures for enhanced oxygen evolution selectivity in seawater splitting. Advanced Functional Materials, 2024, 34(24): 2315949

[S14] Chen B J, Humayun M, Li Y D, et al. Constructing hierarchical fluffy CoO−Co_4N@NiFe-LDH nanorod arrays for highly effective overall water splitting and urea electrolysis. ACS Sustainable Chemistry & Engineering, 2021, 9(42): 14180–14192

[S15] Li Y Y, Guo H R, Zhang Y, et al. Hollow Mo-doped NiS_x nanoarrays decorated with NiFe layered double-hydroxides for efficient and stable overall water splitting. Journal of Materials Chemistry A, 2022, 10(36): 18989–18999

[S16] Cao Y H, Li Z, Yin X L, et al. Electronic modulation and reaction-pathway optimization on three-dimensional seaweed-like NiSe@NiMn LDH heterostructure to trigger effective oxygen evolution reaction. Journal of Colloid and Interface Science, 2024, 658: 528–539

[S17] He L X, Wang N, Sun B L, et al. A low-cost and efficient route for large-scale synthesis of $NiCoS_x$ nanosheets with abundant sulfur vacancies towards quasi-industrial electrocatalytic oxygen evolution. Journal of Colloid and Interface Science, 2023, 650: 1274–1284

[S18] Rajendiran R, Muthuchamy N, Park K H, et al. Self-assembled 3D hierarchical $MnCO_3$/NiFe layered double hydroxides as a superior electrocatalysts for the oxygen evolution reactions. Journal of Colloid and Interface Science, 2020, 566: 224–233

[S19] Feng Y Q, Wang X, Huang J F, et al. Decorating CoNi layered double hydroxides nanosheet arrays with fullerene quantum dot anchored on Ni foam for efficient electrocatalytic water splitting and urea electrolysis. Chemical Engineering Journal, 2020, 390: 124525